Journal of Environment and Earth Science
ISSN 2224-3216 (Paper) ISSN 2225-0948 (Online)
Vol.4, No.2, 2014
www.iiste.org

Utilization of Landsat 7 ETM+ Multispectral Data and ASTER-GDEM in Geological Investigation and Alteration Mapping around Yankara-Dan Sabo-Takulawa Area within Wonaka Schist Belt, Northwestern Nigeria

A.K Amuda[1]*, U.A Danbatta[1] and T. Najime[1]
Deparment of Geology, Ahmadu Bello University, Zaria, Nigeria.
*E-mail of the corresponding author: akabdulgafar@abu.edu.ng

Abstract
The study area forms part of the Precambrian to Early Paleozoic Nigerian Basement complex. ASTER-GDEM image draped on topographical map aided 3-D perspective view of physiographic features in the area. The Landsat ETM+ remote sensing data has suitable spectral and spatial properties that aided lithological and alteration mapping. Spectral transform approaches, consisting of band ratio (BR), principal component analysis (PCA), False Color Composition (FCC), and Feature Oriented Principal Component Selection (FOPC) were utilized. Prior to image processing, the ETM+ data were also subjected to image pre-processing. The results show that BR, PCA and FCC images discriminates the granitic rocks and metasediments. Color melange including ETM+ (7/4+4/3+5/7, 3/1+5/7+4/54 and 5/7+3/2+4/5) discerned highly altered zones and iron rich minerals. Colour composite (Kauffman ratio) and FCC show vegetation preponderance mostly on metasediments. Alteration of hydroxylated-silicate rocks are distinct with PCA. Hydroxyl minerals with marked oxidization and argillization are more recognizable with FOPC (Crosta technique) than PCA techniques. Structurally, the spectral responses distinctly show symmetrical M-shape fold pattern in granitic rocks that span within the southeastern part of the area. The area also exhibit highest lineament density. Nearly N-S lineament trend corresponding to imprints of Pan-African Orogeny predominates.
Keywords: Alteration mapping, Band ratioing, Lineament density, Lithology

1. Introduction

The surface area of Nigeria 923,768 km^2 is covered in nearly equal proportions by crystalline rocks and sedimentary rocks. The crystalline rocks are further divided into three main groups viz: (i) the Basement Complex; (ii) the Younger Granites and (iii) Tertiary – Recent volcanics.The basement rocks are believed to be the results of at least four major orogenic cycles of deformation, metamorphism and remobilization corresponding to the Liberian (2,700 Ma), the Eburnean (2,000 Ma), the Kibaran (1,100 Ma), and the Pan-African cycles (600 Ma) (Rahaman, 1988; Ogezi, 1977; Ajibade *et al.*, 1987). Each of the thermotectonic events produced characteristic imprints on the basement rocks. However, the Pan-African event was so pervasive that it obliterated most of the structures of the earlier events, leaving only their traces (McCurry, 1976; Rahaman, 1976; Grant, 1978). The predominant trend of structures on the basement is in the N-S direction with some variation in NW-SE and NE-SW direction (Oluyide 1988, Olujide and Udoh, 1989).

The Nigerian Basement Complex forms a part of the Pan-African mobile belt and lies between the West African and Congo Cratons (Fig. 1) and south of the Tuareg Shield (Black, 1980). The study area falls within Wonaka Schist belt and forms part of the Precambrian to Early Paleozoic Nigerian Basement complex. The basement is characterised by 12 synclinorial belts (Fig. 1) of low grade metasediments downfolded into high grade gneisses and migmatites, the whole intruded by batholitic granites (McCurry and Wright, 1977). Ajibade and Fitches (1988) reported that the metasedimentary and metavolcanic rocks which form the schist belts appear to be dominantly restricted to the western half of the country (Fig. 1). The Wonaka Schist belt is distinctive in composition and metamorphism with a monotonous span of biotite schist (Harper *et al.*, 1973; Turner, 1983). The study area covers an area of 770 km^2 and is bounded by longitudes 11^{o}45′ N and 12^{o}00′ N and latitudes 7^{o}00′ E and 7^{o}15′ E (Fig. 1).

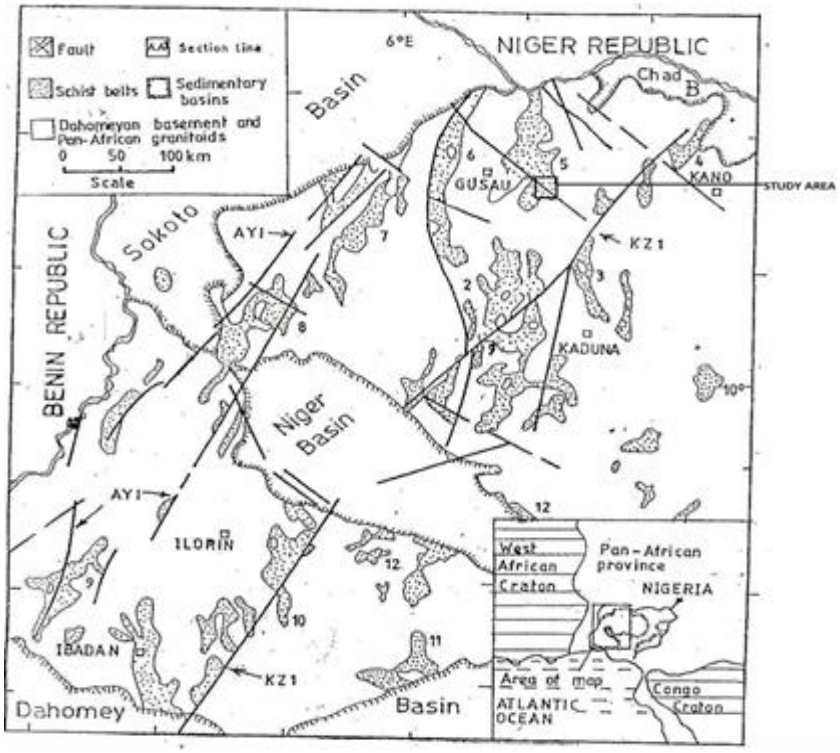

Fig. 1: Study area within a simplified geological map of the Northern and Southern part of the Western half of Nigeria, showing the distribution of the schist belts and the locations of major lineaments (modified after the Geological Survey of Nigeria map, 1994 in Danbatta, 2008). The schist belts are 1. Zungeru-Birning Gwari, 2. Kushaka, 3. Malumfashi, 4. Kazaure, 5. Wonaka, 6. Maru, 7. Anka, 8. Zuru, 9. Iseyin-Oyan River, 10. Ife-Ilesha, 11. Igarra-Kabba-Lokoja, 12. Toto, AYI = Anka-Yauri-Iseyin fault system. KZI= Kalangai-Zungeru-Ifewara fault system. Inset is location of Nigerian sector of the Pan-African Province of West Africa.

Remote sensing (RS) techniques play an important role in mapping programs (Farina *et al*. 2005). It has always been difficult to map lithologies and alteration zones in inaccessible mountain and forest terrain. The accuracy of lithological boundaries and structural details are not usually precise in such maps. Physical investigation of every outcrop in most cases is hindered by inaccessibility. At this juncture, the potential of RS cannot be over emphasized. The greatest advantage of RS is the synoptic view that it provides. It gives a regional and integrated perspective of interrelations between various land features. There is a relative increase in use of RS technique primarily because new satellite images with better spatial and spectral resolutions (e.g Landsat 5 TM, Landsat 7 ETM+, SAR etc) coupled with development of software (PCI-Geomatica, ENVI, ArcGIS etc) technology for spectral image processing/enhancements.

The existing multi spectral satellite systems are designed to investigate natural resources with special focus on vegetation coverage, lithology and mineral exploration (Crippen and Blom, 2001; Yousif and Shedid, 1999). In the regions where bed rock is exposed multi-spectral RS is useful for mapping lithology and alteration zones. Subsequent Studies, in South-West USA and elsewhere (Podwysocki *et al*., 1983; Abrams, 1984) have confirmed that areas of hydrothermal alterations may be distinguishable using the ratio of TM band 5 and 7. Also it is evident that the spectral characteristics of TM bands are suitable for mapping lithology. Bands of Landsat 7 ETM+ (Table 1) offer a unique spatial, spectral and radiometric resolution (Jenson and Domingue, 1988).

An Enhanced Thematic Mapper Plus (ETM+) sensor, which includes an eighth (panchromatic) band with a spatial resolution of 15 meters, was onboard Landsat 7 when it successfully launched in 1999.

Table 1: Landsat TM and ETM+ (after Sabins, 1999)

Spectral Sensitivity (μm)	**Spatial Resolution (m)**
0.522 – 0.90 (panchromatic)	15
0.45 – 0.52 (visible blue)	20
0.52 – 0.60 (visible green)	30
0.63 – 0.69 (visible red)	30
0.76 – 0.90 (near IR)	30
1.55 – 1.75 (mid IR)	30
10.40 -12.50 (thermal IR)	120 (Landsat 4-5), 60 (landsat 7)
2.08 – 2.35 (mid IR)	30

RS is a valuable tool for mapping the local fractures and lineaments that may control mineralization (e.g. Abdelsalam *et al*., 2000). Also, RS is valuable for mapping hydrothermally altered minerals that have distinct absorption features (Hunt, 1979). Abdelsalam *et al.*, (2000) utilized the 5/7, 4/5 and 3/1 band ratios image in Red, Green, Blue (RGB) for mapping the Beddaho alteration zone in northern Eritrea. Ramadan *et al.*, (2001) mapped the alteration zones associated with gold-bearing massive sulphide deposits, Allaqi suture, South Eastern Desert of Egypt, using Landsat TM color composite ratio images. Ramadan and Kontny (2004), utilized Landsat TM band ratios to study Shalatein District, South Eastern Desert of Egypt, and detected two types of alteration zones controlled by NW-SE structural trend. Salem (2007) utilized the remote sensing techniques for geology and gold mineralization at al Faw - Eqat area, South Eastern Desert, Egypt. He used the PCA and band ratios techniques in tracing the alteration zones possibly gold bearing in the study area.

Table 2: Summary of literally known band ratio composites.

RGB display of respective TM band Ratios	Red Correspondent	Green Correspondent	Blue Correspondent	Extra	Reference
5/7; 3/2; 4/5	Clay rich areas	FeO rich areas		Yellow, orange areas both clay and FeO rich	Abrahs *et al.*, 1983
7/4; 4/3; 5/7	Minerals containing iron ions	Vegetated zones	OH/H_2O-SO_4 or CO bearing minerals		Kauffman 1985
3/4; 5; 5/7				FeO as apricot yellow and the background as sky blue	Jingyuan and Xucman, 1991
5/7; 5/4; 3/1	Clay minerals	Iron minerals	Ferric oxides		Chical-Olmo 2002
3/1; 5/7; 4/5				Highly altered zones dark-blue to violet-blue	Abdelhamid and Rabba 1994

Remote sensing is not limited to direct geology applications - it is also used to support logistics, such as route planning for access into a mining area, reclamation monitoring, and generating base maps upon which geological data can be referenced or superimposed (Joshi, 1999).

In Nigeria, not much has been achieved using geospatial technology in lithologic mapping and mineral exploration. Much of the work on remote sensing has been targeted at hydrogeological applications (Bala, 1997; Bala *et al*., 2000a; Goki *et al.*, 2005; Anudu *et al.*, 2011). Talaat and Mohammed (2010) used digitally processed Landsat 5 imageries to characterize gold mineralization in Garin Hawal area, NW Nigeria. Abubakar (2012) used a combined Landsat and aeromagnetic map to map and delineate structures in the kushaka Schist Belt. Kankara (2011) used Landsat imagery to map mineral deposits in some areas of Kaduna States of Nigeria. As part of an on-going research on petrological and mineral resource potential of the study area, present work utilizes ASTER-GDEM and ETM+ images covering the study area to enhance lithologic mapping and delineate alteration zones.

2. Methodology

A detailed review of relevant literature on geology and application of remote sensing in Nigerian Basement Complex. Advanced Spaceborne Thermal Emission and Reflection (ASTER) Global Digital Elevation Model (GDEM) was draped on topographic map for 3D physiographic view of the study area. Also, subsets of the ETM+ scene (Path 189/Row 052, acquired on October 19, 1999) were processed using the ENVI 4.5 image processing and analysis software. ArcGIS 9.1 and PCI Geomatica 9.1 software packages are both used in digital

processing, spectral enhancement, spectral classification and geospatial analysis of the produced enhanced images for lithological classification and identifying alteration halos of mineralized bodies. Image processing techniques including Band Ratioing (BR), Principal Component Analysis (PCA), False Color Composition (FCC), and Feature Oriented Principal Component Selection (FOPC) have been applied on TM bands 1, 2, 3, 4, 5 and 7 for reconnaissance mapping of the lithological units, structures and alteration zones in the study area.
The PCI-Geomatica software was used for digital image processing. This provided useful lithological, structural and mineral information with methodology shown in Fig. 2 below.

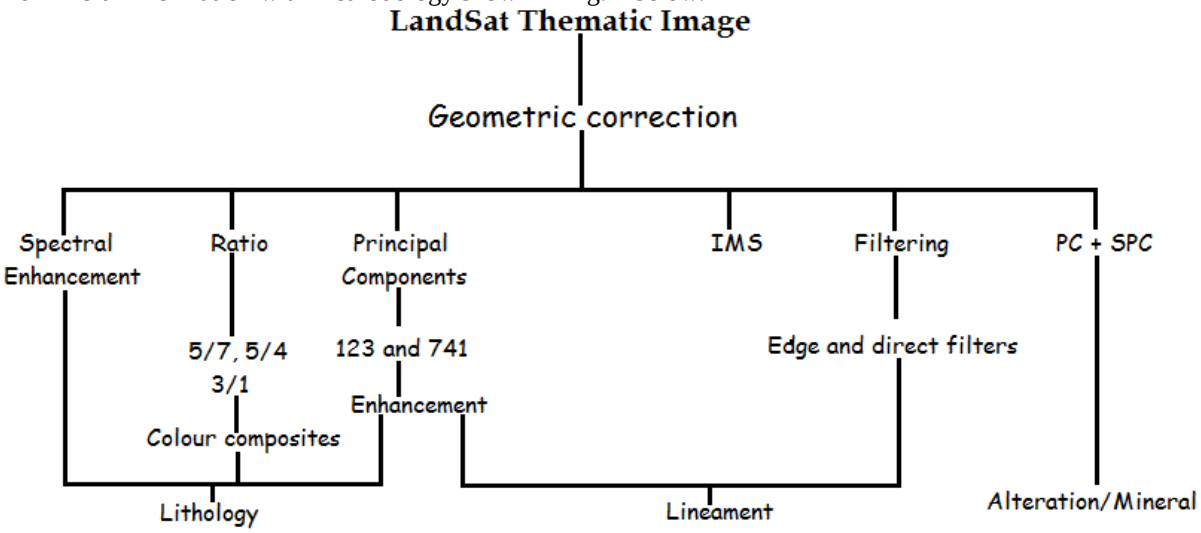

Fig. 2: Methodology diagram for processing and enhancement of LandSat Thematic Image.

3. Results and Discussion

3.1 Digital Elevation Model

Digital elevation model of the study area was draped on topographic map to have a 3-D perspective view of physiographic features in the study area. Atlas shaded view displayed topographic variations with color (Fig. 3.1). The highest outcrop (relief) lies at the northwestern edge of the study area. Other smaller outcrops and features like the major rivers and their tributaries, access roads (main and minor) are seen.

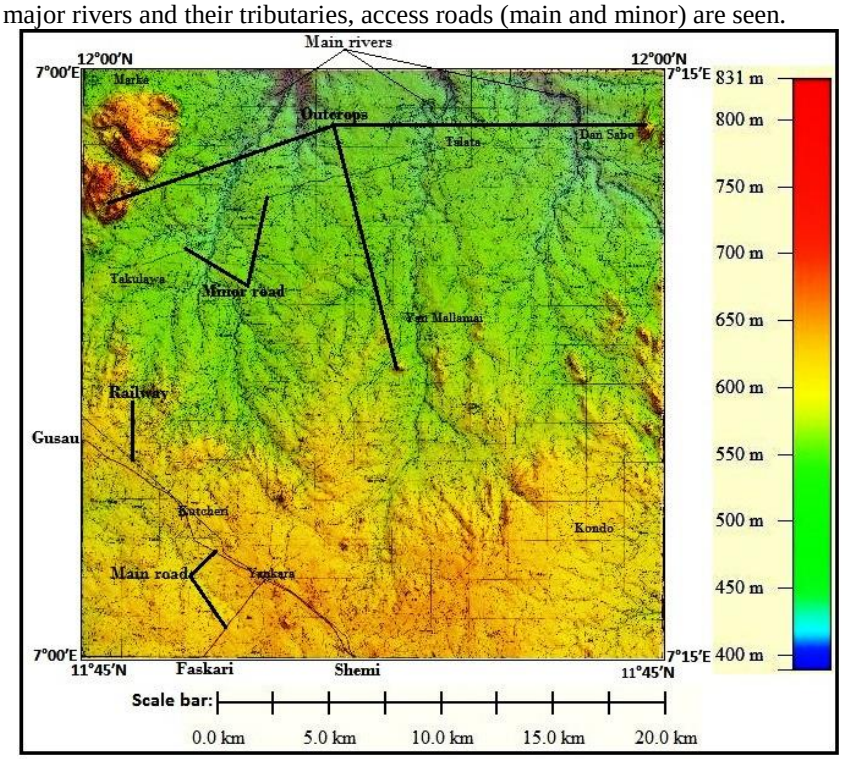

Fig. 3: ASTER GDEM draped on topographic map of the study area.

3.2 Band Ratioing

The digital number (DN) in one band was divided by the corresponding DN in another band for each pixel, stretching the result value and plotting the new values as an image. This method is used by (Weissbrod *et a*l. 1985; Cappiccioni *et al.* 2003; Edgardo 1992) to extract spectral information from multi-spectral imagery. Color Composite of ratio images 3/1, 5/7 and 3/5 (RGB) express more geological information and provide higher contrast between units than the conventional color images. The band ratio transformation of TM data is useful for qualitative detection of hydrothermal altered minerals (Di Tommaso and Rubinstein, 2007), and also has wide acceptance in geological mapping (e.g., Madani *et al.*, 2003; Qiu *et al*., 2006).

In this study, the ETM+ band ratio (5/7) images were used to identify granitic lithology which had bright white to faint grey tone. The metasediments display light to dark grey colour (Fig. 4a). Reverse of band ratio 5/7 was observed for granitoid rocks on the ETM+ band ratio 3/1 as they mainly displayed dark grey tone (Fig. 4b). A similar image tone was also noted for granitods in the South Eastern Desert, Egypt (Zoheir and Enam, 2012).

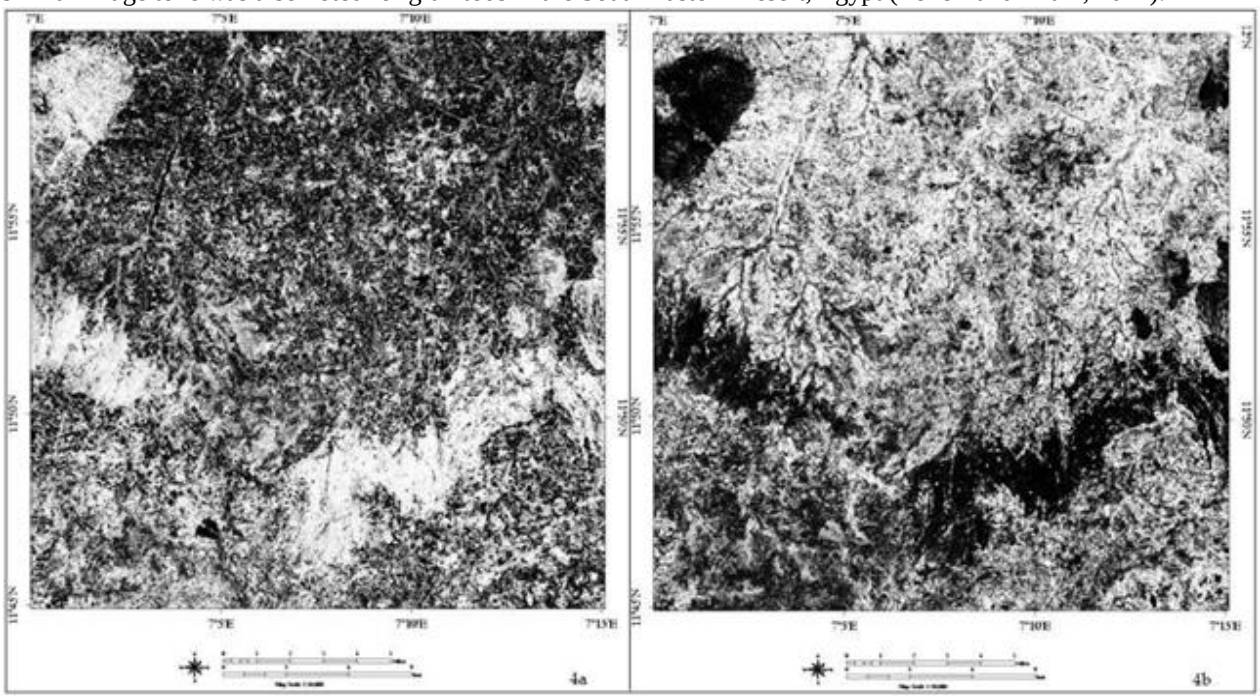

Fig. 4: (a) ETM+ band ratio 5/7 of the study area showing granite and gneisses with high tone of white to mist grey. (b) ETM+ band ratio 3/1 of the study area showing granite and gneisses show dark grey tone.

Tone of band ratio 5/4 is similar to 3/1 except that the dark grey is intermediate in places. Alluvium on terrace around stream channels had bright white tone. The metasediments are generally light toned (Fig. 5). Shalaby *et al.* (2009) also used the ratio to discriminate between the mafic/ultramafic rocks (bright tone) from granitoids (dark tone) in granitic plutons in eastern Egypt.

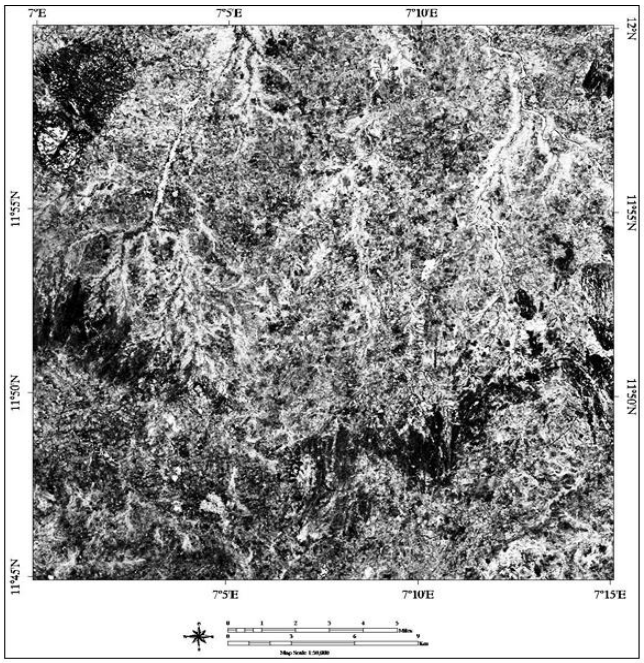

Fig. 5: ETM+ band ratio 5/4 of the area showing granitic rocks with intermediate dark to pale grey tone.

3.3 Chica-Olmo and Kaufmann ratio

In 2002, Chica-Olmo developed a ratio (Chica-Olmo ratio) which include the combination of ETM+ band ratios 5/7 (Red), 5/4 (Green) and 3/1 (Blue) sequence as images for the detection of hydrous minerals and iron-rich zones. This ratio was adopted in the study area. Red correspondences are for clay minerals (alteration from feldspars) while iron minerals and ferric oxides are green and blue respectively (Chica-Olmo, 2002). The quartzofeldspathic granites displayed red tone while the metasediments with iron and ferric oxides are green. Clear green signature indicating presence of iron minerals are also observed on some parts of Kuruku hill in the northwestern part of the study area (Fig. 6a).

Also, Color composite created by band ratio 7/4, 4/3 and 5/7 displayed as RGB respectively of (Kaufmann, 1988) was adapted. Consequently red color represents the minerals containing iron ions; green represents the vegetated zones and blue represents OH/H_2O-, SO_4- or CO bearing minerals in rocks and soils (Kauffmann, 1988). Minerals containing iron ion are prevalent (Fig. 6b).

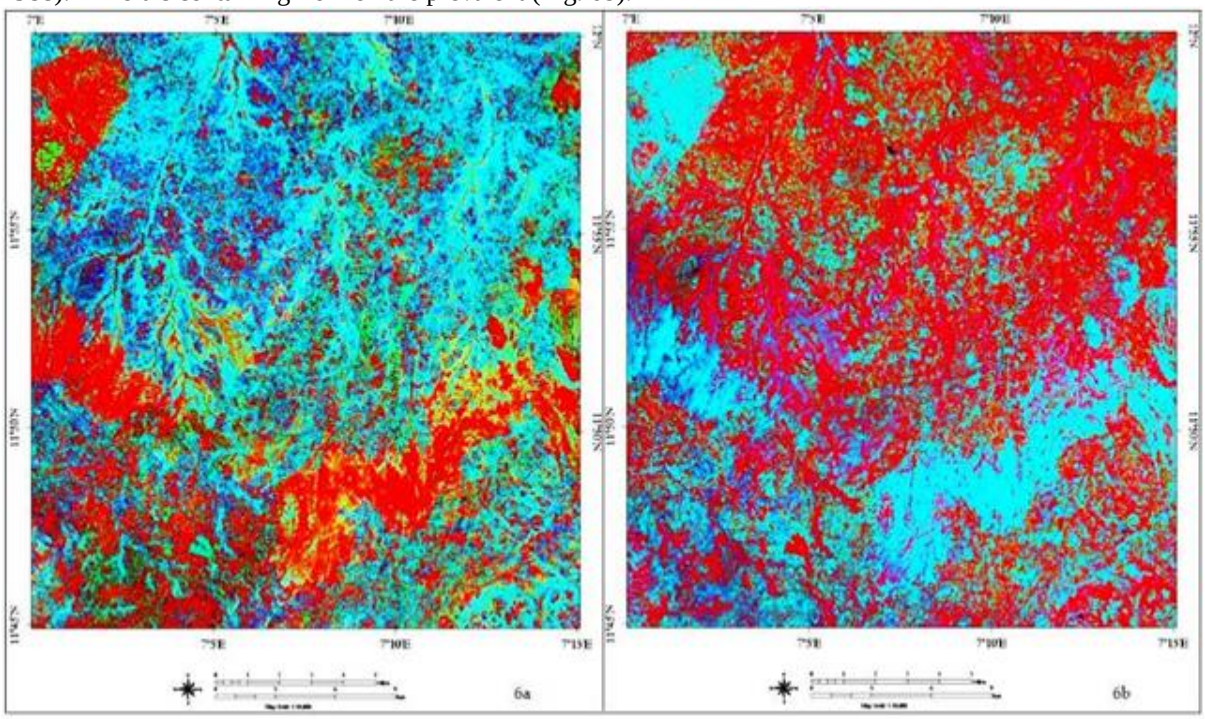

Fig. 6: (a) Colour composite (Chica-Olmo ratio) which include the combination of ETM+ band ratios 5/7 (R) for granitic rocks, 5/4 (G) for iron minerals and 3/1 (B) for ferric oxides. (b) Colour composite (Kaufmann ratio) which include the combination of ETM+ band ratios 7/4, 4/3 and 5/7 displayed as RGB showing areas of mineral alteration.

3.4 Abdelhamid/Rabba and Abrams ratio

The color composite of ETM+ 3/1, 5/7 and 4/5 band ratios (Abdelhamid and Rabba ratio) assigned to RGB channels respectively clearly displays the distribution of highly altered zones in dark-blue to violet-blue colours (Abdelhamid and Rabba, 1994) (Fig. 7a).

Also, Band ratios of 1.65 / 2.2 µm, 0.66 / 0.56 µm and 0.83 / 1.65 µm which correspond to 5/7, 3/2 and 4/5; are selected for the red, green and blue channels. Iron oxide-rich areas are displayed as green due to the presence of ferric iron charge transfer band in the ultraviolet, and clay-rich areas are displayed as red, due to the presence of the hydrous minerals absorption band near 2.2 µm. Yellow or orange areas represent the areas where both clay and iron oxide minerals are present (Abrams *et al.*, 1983).

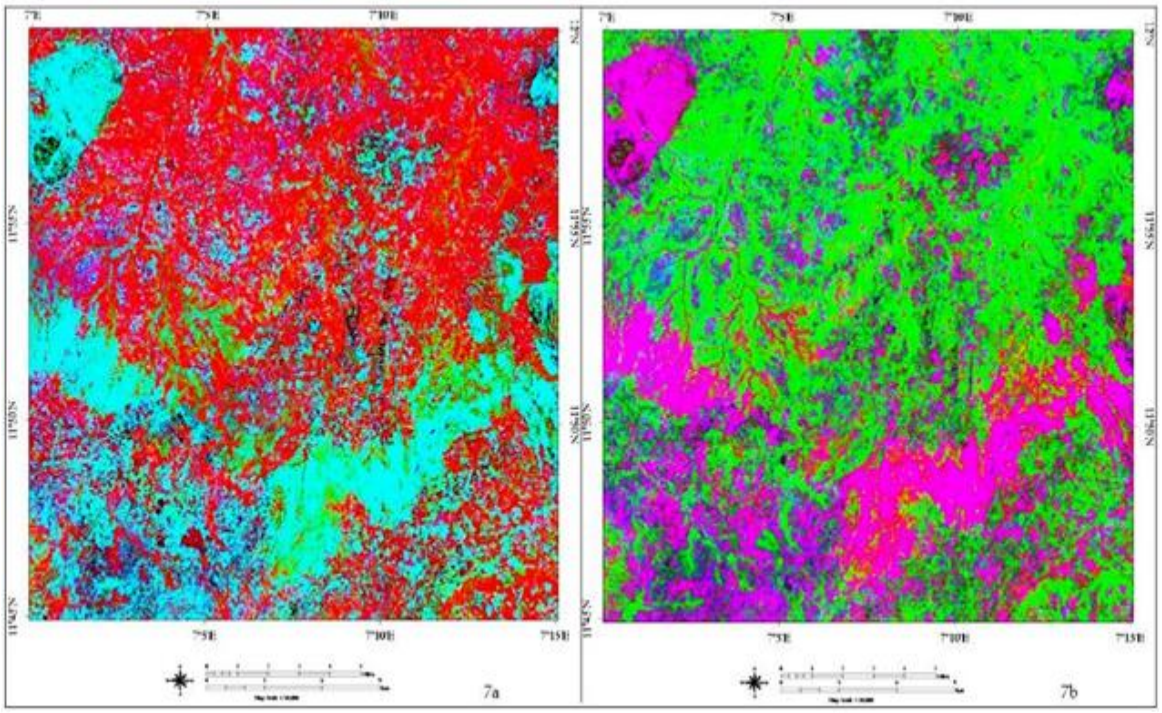

Fig 7: (a) Colour composite (Abdelhamid and Rabba ratio) which include the combination of ETM+ band ratios 3/1, 5/7 and 4/5 displayed as RGB showing highly altered areas. (b) Colour composite (Abrams ratio) which include the combination of ETM+ band ratios 5/7, 3/2 and 4/5 displayed as RGB showing hyrothermally altered areas with yellow to orange colour.

3.5 Principal Component Analysis (PCA) and False Colour Composite (FCC)

PCA is a multivariate statistical method which predicts whether the target material is represented as bright or dark pixels in the different principal components according to the magnitude and sign of the Eigenvector loadings (Jenson, 1996). The advantage of principal component analysis is that most information within all the bands can be compressed into much smaller number of bands with little loss of information. Thus, as you move from the first to the last principal component band the amount of information carried reduces. Principal component analysis of ETM images has been shown to be a successful tool in minimizing vegetation effects (Loughlin, 1991).

In present work, RGB colour composite was generated using band combinations: 1, 2, and 3 for lithology and alteration mapping. In the composite, the granitic rocks are mainly depicted by blue to light red colour tones; the undifferentiated metasediments as light green to light blue colour, respectively. A symmetrical M-shape folding was observed in granitic rocks that tapered from the east down in the south eastern part of the study area (Fig. 8a).

All known mineralization have been mapped in a distinct yellowish colour against bluish-red country rocks (Kenea, 1996). Presence of yellowish hue which coincidentally mark areas of placer gold occurrences reported north of Kutcheri (Amuda *et al.*, 2013). Yellowish hue suggests the dominance of hydroxylated-silicates in mineralization and could also be followed to discern insitu altered rocks (Kenea, 1996) (Fig 8a).

The colour of a target in the displayed image does not have resemblance to its actual colour. The resulting

product is known as a "False colour composite". There are many possible schemes of producing false colour composite images. In this study, Landsat band-7, 4, 1 was assigned to Red, Blue and green channels to produce a False composit colour.

FCC image efficiently discriminate granitoid from metasedimentary rocks. Granitic rocks are dark green to brown, whereas metasediments occur as pale green. The vegetation cover appears crome green (Fig. 8b).

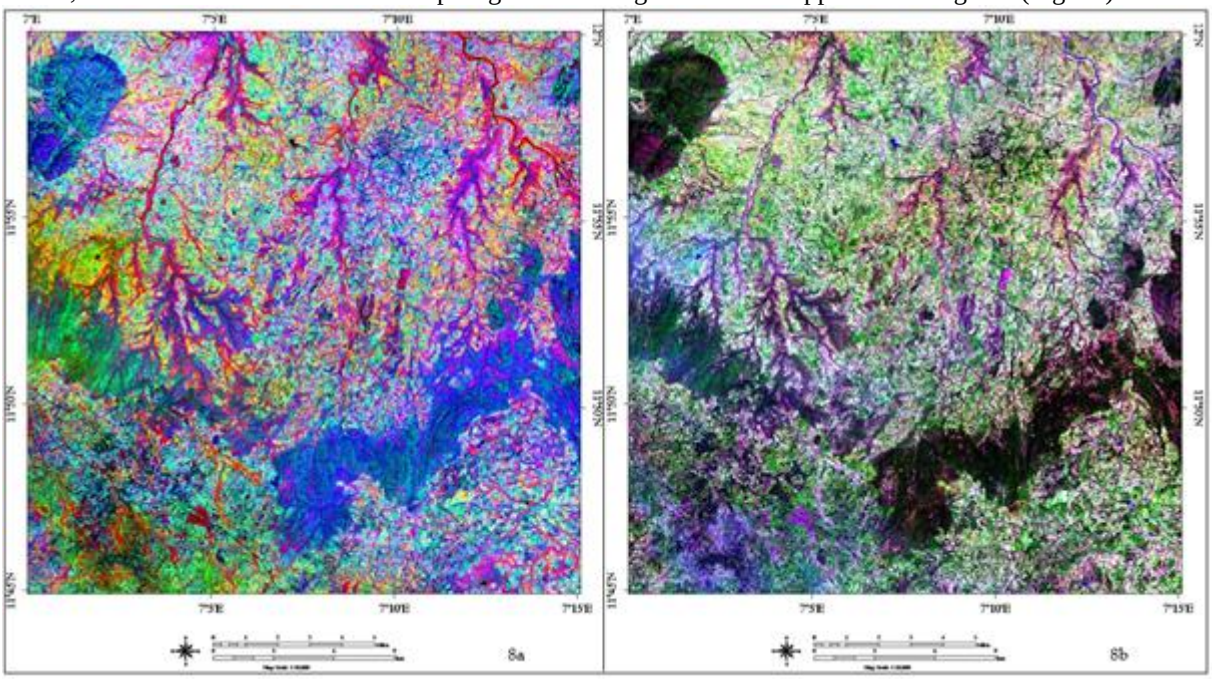

Fig. 8: (a) PCA bands of ETM+ PC1,PC2,PC3 dicriminating lithology and alteration in hydroxylated-silicates rocks. (b) FCC bands of ETM+ 7,4,1 dicriminating lithology and vegetation cover.

3.6 Crosta Technique

The principal component transformation is a multivariate statistical technique that selects uncorrelated linear combinations (eigenvector loadings) of variables in such a way that each successively extracted linear combination or principal component (PC) has a smaller variance (Singh and Harrison, 1985). Crosta technique is also known as feature oriented principal component selection. Through the analysis of the eigenvector values it allows identification of the principal components that contain spectral information about specific minerals, as well as the contribution of each of the original bands to the components in relation to the spectral response of the materials of interest. This technique can be applied on four bands of ETM+ data and indicates whether the materials are represented as bright or dark pixels in the principal components according to the magnitude and sign of the eigenvector loadings (Armenta and Ledesma, 2010).

The principal component transformation (eigenvectors and eigenvalues) was performed by using four ETM+ bands as input bands (bands 1, 4, 5 and 7) for hydroxyl minerals. The study of Spectral reflectance curves for clay minerals indicates that the clay minerals have absorption in band 7 and Reflection in band 5. These bands have higher loadings in PCA, but with opposite sign. PC4 has a negative contribution of band 5 and positive contribution of band 7. Therefore, pixels that have hydroxyl minerals will be darker in the final hydroxyl image. But in order to show the areas with hydroxyl minerals in bright pixels an inverse of this PC is obtained by using PC4 (Fig. 9a).

The same technique is used on 4 Bands (Bands 1, 3, 4, and 5) to enhance iron oxides. According to reflectance of iron oxides, these minerals have absorption feature in band 3 and strong reflection in band 1 (Armenta and Ledesma, 2010).. These two bands have, therefore, higher loadings through PC analysis, but again with opposite sign, and the pixels with more abundances of iron oxides minerals will be darker in the final image. In order to show the areas with iron oxide minerals in bright pixels, an inverse of this PC is obtained by using PC3 (Fig. 9b).

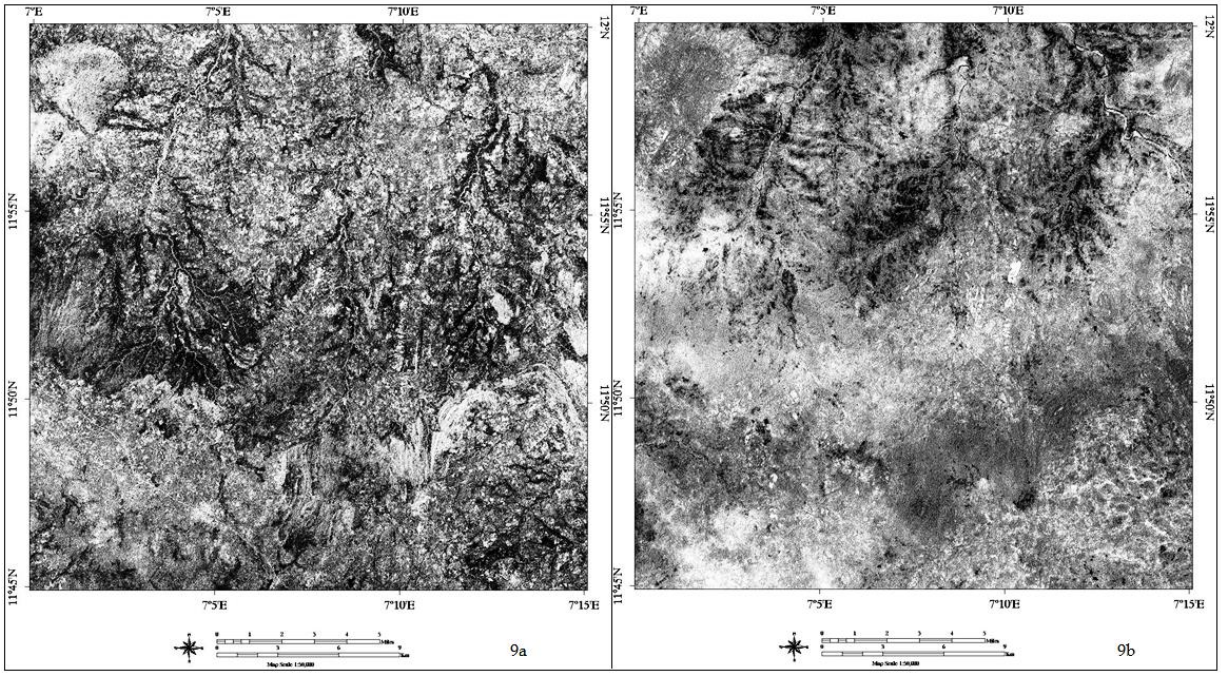

Fig. 9: (a) H image (bands 1, 4, 5 and 7) showing areas of hydroxyl (OH) minerals in the study area with high tone. (b) F image (bands 1, 3, 4 and 5) showing areas of iron oxide minerals with high tone.

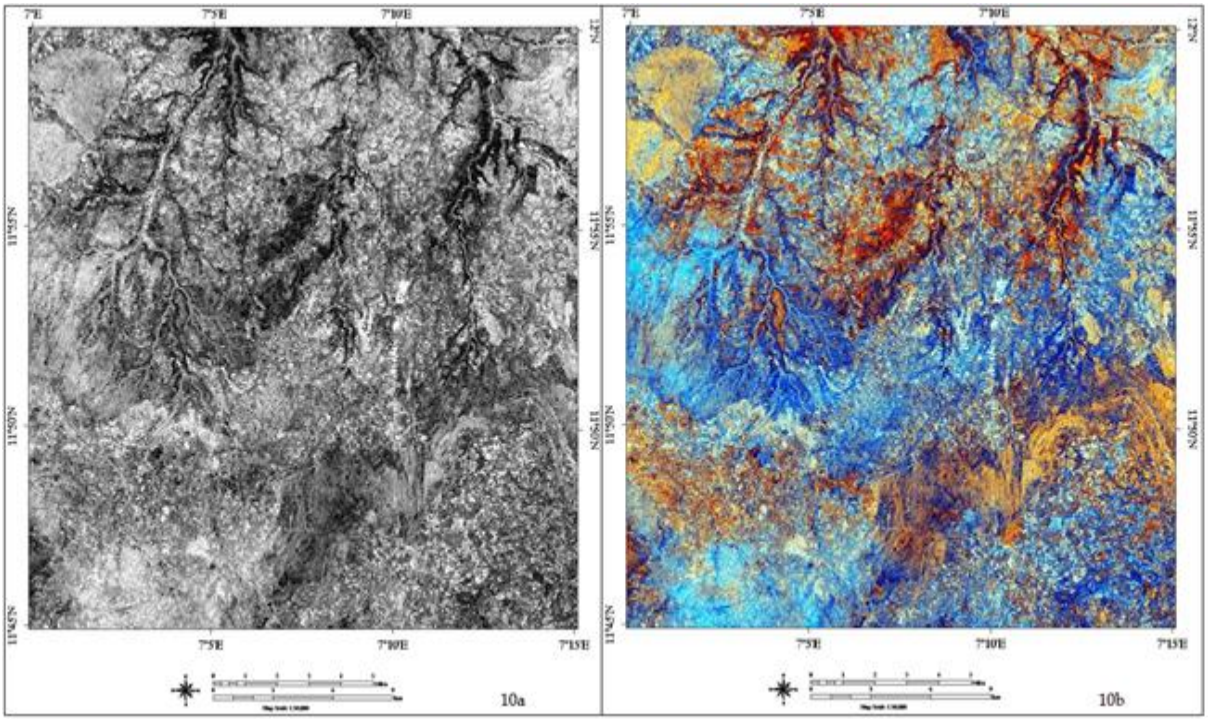

Fig. 10: (a) H+F image showing areas of hydroxyl and iron oxide minerals in the study area with bright tone. (b) Crostal image (composite of H, H+F and F) displayed respectively in RGB channels showing areas oxidized and argillized (white specks), oxidized (bright blue) and medium to dark brown areas dominated by hydroxyl minerals.

For applying Crosta techniques, the information stored on the hydroxyl (H) and iron-oxide (F) images are combined to produce a map displaying the pixels with anomalous concentrations of both hydroxyls and iron-oxides as the brightest (Loughlin 1991). This new image is called H+F image (Fig 10a).

By using the Crosta H, H+F and F images, where they are stretched in desired combinations, colour composites are prepared. Displaying of the Crosta images of H, H+F and F in RGB channels returns a dark bluish colour

composite image on which alteration zones are unusually bright (Fig. 10b). Specks of white pixels within alteration zones are the areas were both iron-stained and argillized. Bright brown to orange zones are more argillaceous than iron-stained; and bright cyan to bluish zones are more iron-stained than argillized (Loughlin, 1991). It is clear from this principal component analysis maps that the altered iron-oxide deposits are abundant within the metasediments which had deep blue tone (Fig. 10b).

3.7 Automatic Lineaments Extraction

The surface expression of geological structures such as, fractures, faults, joints, shear zones and foliations are shown in the form of lineaments on airborne and orbital remote sensing data (Koch and Mather, 1997). Automatic lineament extraction from remote sensing data is an important approach for regional structural studies and mineralization. Recognition of lineaments has been used for mineral exploration studies (Rowan and Bowers, 1995).

The lineaments analysis step aims to understand the relationship between the lineament trends (faults) as the main structural element affecting the rock units exposed at the study area. Landsat panchromatic image (15m) was prepared to conduct this test under the default parameters of LINE module of PCI software (Table 3).

Table 3: Default parameters for LINE module for linearment extraction.

Parameter	**Default**
Filter radius (pixel)	10
Edge gradient threshold	40
Curve length threshold (pixel)	30
Line fitting error threshold(pixel)	3
Angular differece threshold(degree)	30
Linking distance threshold (pixel)	20

Automatic lineaments extraction from Landsat panchromatic image was run with three major steps: 1) edge detection, 2) threshold and 3) lineaments extraction. The main lineament trends automatically extracted in the study area show a pattern (Fig. 11a).

The lineament frequency rose diagram mainly trend in NNE-SSW, NE-SW, NNW-SSE. Nearly E-W trend and other directions are subordinate direction (Fig. 11b). The dominant trend direction (nearly N-S) is consistent with regional structures resulting from Pan African Orogeny that obliterated most other pre-Pan African deformations. Also, there is concordant relationship between these lineaments and drainage pattern system distribution especially with first to second river orders from topographic map

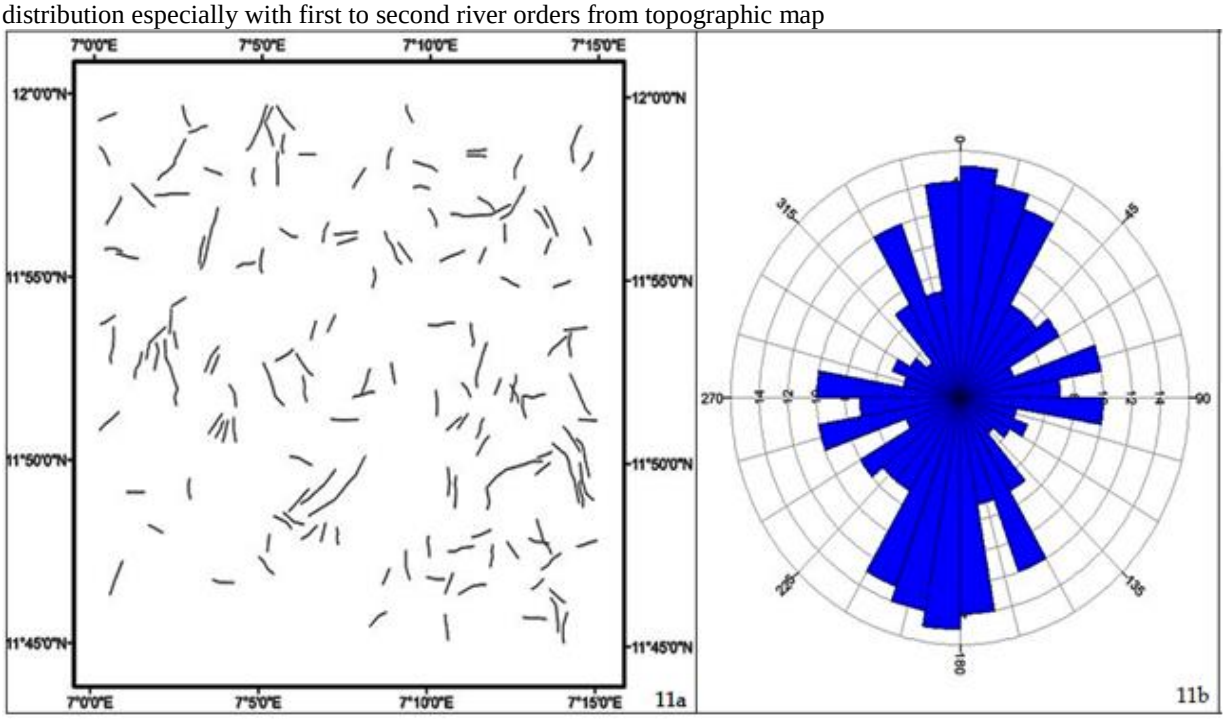

Fig. 11: (a) Automatic extracted lineament trends (default setting) of structures in the study area. (b) Rose (azimuth-frequency) diagram of lineaments orientations

On a lineament density map, the lineaments extent and intensity is highest within the southeastern part (Fig. 12) around Kauro corresponding to the area occupied by the folded granitic rock.

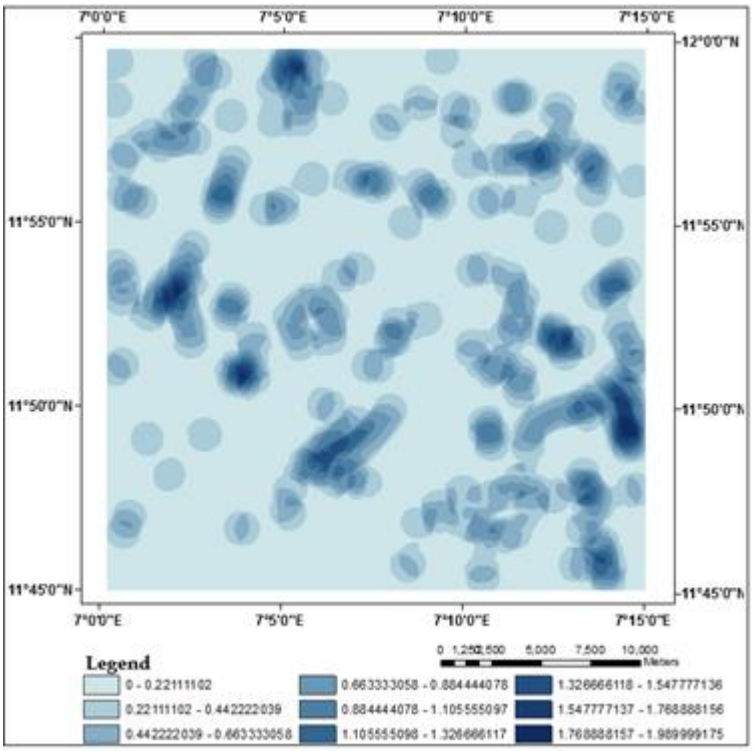

Fig. 12: Lineament density map of the study area.

4. Conclusion

This study showed that Remote Sensing techniques are an efficient tool for geological mapping. Advanced Spaceborne Thermal Emission and Reflection-Global Digital Elevation Model aided 3-D visualization of features. Different processing techniques were applied to the LandSat ETM+ images to discriminate the lithological units, alterations and lineaments. The Band ratioing, Principal Component analysis and False Colour Composites allowed broad discrimination of lithologies. Detection of altered areas, iron rich and hydroxylated-silicate minerals were discerned with Principal Component analysis and Feature Oriented Principal Components. Nearly N-S Lineament trend concordant with regional Pan African Orogeny deformation trand predominates.

5. Acknowledgement

The authors acknowledged free access to LandSat ETM+ bands through Global Land Facility Cover of University of Maryland, United States of America. The first author also acknowledges assistance of Mr. W. T Andongma who put me through basics of processing and analysis of Multispectral data.

References

Abdelhamid, G. and Rabba, I. (1994). An investigation of mineralized zones revealed during geological mapping, Jabal Hamra Faddan-Wadi Araba, Jordan, using Landsat TM data. *International Journal of Remote Sensing*, volume 15, Number 7, pages 1495 – 1506.

Abrams, M.J., Brown, D., Lepley, L. and Sadowski, R. (1983). Remote sensing for porphyry copper deposits in southern Arizona. *Economic Geology*, Volume 78, pages 591–604.

Abrams, M.J. (1984). LandSat 4, Thematic Mapper and Thematic Mapper Simulator data for a Porphyry Copper Deposit. Photogrammetric Engineering and Remote Sensing, Volume 50, pages 1171-1173.

Abrams, M.J., Rothery, D.A. and Pontual, A. (1988). Mapping in the Oman ophiolite using enhanced Landsat Thematic Mapper images. *Tectonophysics* 151, 387–401.

Abdelsalam, M.G., Stern, R.J and Berhane, W.G. (2000). Mapping gossans in arid regions with Landsat TM and SIR-C images: The Beddaho alteration zone in northern Eritrea; *Journal of African Earth Science*, Volume 30, Number 4, pages 903–916.

Abubakar, Y.I. (2012). An Integrated Technique in Delineating Structures: A Case Study of the Kushaka Schist Belt Northwestern Nigeria. *International Journal of Applied Science and Technology.* Vol. 2, No. 5.

Ajibade, A.C. and Fitches, W.R. (1988). The Nigerian Precambrian and the Pan-African Orogeny. *A publication*

of the Geological Survey of Nigeria.
Ajibade, A.C., Rahaman, M.A., and Woakes, M. (1987). Proterozoic crustal development in the Pan-African Regime of Nigeria. ILP Working Group 3 Mid-term Report.
Anudu, G.K., Obrike, S.E., Onuba, L.N. and Ikpokonte, A.E. (2011). Hydrochemical Analysis and Evaluation of Water Quality in Angwan Jeba and its Environs, Nasarawa State, Northcentral Nigeria. *Research Journal of Applied Sciences.* Volume 6, Number 2, pages 128-135.
Armenta, R.J.R., Ledesma, P.R.M (2010): Techniques for enhancing the spectral response of hydrothermal alteration minerals in Thematic Mapper images of Central Mexico, *Intl. Journal of Remote Sensing.*
Amuda, A.K., Danbatta, U.A., Najime, T. (2013): Geology and gold mineralization around Kutcheri, Northwestern Nigeria. *IOSR Journal of Applied Geology and Geophysics. Volume 1, issue 6, pages 18-24.*
Bala, A. E.(1997): Remote Sensed Groundwater Potential of The Basement Complex Around Dutsinma, Katsina state, Nigeria. Unpublished MSc. Theses, Inter University Program in water resources Engineering , Vrije Universiteit, Brussels, 70 pages
Bala, A. E., Batelaan, O. and De Smedt, F. (2000a): Using Landsat 5 Imagery in The Assessment of Groundwater Resources In The Crystalline Rocks Around Dutsinma, northwestern Nigerian. *Journal of Mining And Geology.* Volume 36, Number 1, pages 85-92.
Black, R. (1980). Precambrian of West Africa. *Episodes 4:3–8.*
Cappaccioni B., Vaselli O., Moretti E., Tassi, F., Franchi R. (2003), The Origin of thermal water from the eastern flank of the Dead Rift Valley, Terra Nova, volume 15 issue3, page145.
Chica-Olmo, M. (2002). Development of a decision support system based on remote sensing and GIS techniques for gold-rich area identification in SE Spain. *Intl. Journal Remote Sensing.*23 (22), 4801–4814.
Crippen, R.E. and Blom, R.G. (2001), Unveiling the lithology of vegetated terrains in remotely sensed imagery. Photogrammetric Engineering and Remote Sensing, 67(8), 935-946.
Danbatta, U.A. (2008). Precambrian crustal development in the northwestern part of Zuru schist belt, northwestern Nigeria. *Journal of Mining and Geology*. 44 (1), pages 45-56 0
Di Tommaso, I. and Rubinstein, N. (2007). Hydrothermal alteration mapping using ASTER data in the Infiernillo porphyry deposit, Argentina. *Ore. Geol. Rev.*, 32: 275-290
Edgardo G. , James J. Hurtak (1992) : Laser Remote Sensing of Forest and Crops in Genetic-Rich Tropical. International Archives of Photogrammetry and Remote Sensing, Vol. XXIX, ISPRS, 7 pages.
Farina, P., Catani, F., Colombo, D., Fumagalli, A., Kukavicic, M., Marks, F., and Moretti, S. (2005). Remote sensing: a tool for landslide investigations at a basin scale. Geophysical Research Abstracts.
Goki, N.G., Oha, I.A., Ike, E.C. and Bala, E.A. (2005). The Use of Digitally Processed Landsat 5 TM Imagery To Map mineralized Pegmatites Around Nassarawa, Central Nigeria. first international Workshop on Geodesy and Geodynamics in Toro, Bauchi State.
Harper, C.T., Sherrer, G., McCurry, P. and Wright, J.B. (1973). K-Ar retention ages from the Pan-African of Northern Nigeria. *Geological Society of Amererica Bulletine 84, 919-926.*
Hunt, G.R. (1979). Near Infrared (1.3–2.4 μm) spectra of alteration minerals – potential for use in remote sensing; *Geophysics* 44 1974–1986.
Jenson, S. and Domingue, J. (1988) Extracting topographic structure from digital elevation data for geographic information system analysis. Photogrammetric Engineering and Remote Sensing, 54 (11).
Joshi, V. (1999). Technical Paper On: Remote sensing and its application. *Final Year, Electronics & Communication. Rishiraj Institute of Technology, Indore.* Pages 1-86
Kankara, I. A. (2011). Mapping of mineral deposits in some areas of Kaduna and Katsina States Nigeria, using geospatial technologies. *Proceedings of First International Geomatics Symposium in Saudi Arabia.*
Kaufmann, H. (1988). Mineral exploration along the Aqaba-Levant structure by use of TM data; concepts, processing, and results. International Journal of Remote Sensing, volume 9, 1639-1658.
Kenea, N.H. (1996): Digital image processing and GIS data integration for geological studies in the Southern Red Sea Hills, Sudan. PhD. Thesis (in preparation). Freie University Berlin, Germany.
Koch, M. and Mather, P.M. (1997). Lineament mapping for groundwater resource assessment: a comparison of digital Synthetic Aperture Radar (SAR) imagery and stereoscopic Large Format Camera (LFC) photographs in the Red Sea Hills, Sudan. Intl. Journal of Remote Sensing, 27, pages 4471–4493.
Loughlin, W.P. (1991). Principal Component Analysis for Alteration Mapping.Photogrammetric Engineering and Remote Sensing, 57, 1163-1169. Thematic Conference on Remote Sensing, Denver, USA.
Madani, A., Abdel Rahman, E.M., Fawzy, K.M. and Emam, A. (2003). Mapping of the hydrothermal alteration zones at Haimur Gold Mine Area, South Eastern Desert, Egypt using remote sensing techniques;*The Egyptian Journal of Remote Sensing and Space Science.* 6 47–60.
McCurry, P. (1976). The geology of the Precambrian to Lower Palaeozoic Rocks of Northern Nigeria – A Review. *In: Kogbe CA (ed) Geology of Nigeria. Elizabethan Publishers, Lagos, pages 15–39.*

Ogezi, A.E.O. (1977). Geochemistry and Geochronology of Basement Rocks from Northwestern Nigeria. Unpublished Ph.D. Thesis, University of Leeds.
Oluyide, P.O. (1988). Structural Trends in the Nigerian Basement Complex. In: P.O. Oluyide Precambrian Geology of Nigeria. *Geol. Surv. Nigeria: Lagos, Nigeria. 93-98.*
Podwysocki, M.H., Segal, D.B. and Abrams, M.J. (1983). Use of multi spectral scanner images for assessment of hydrothermal alteration in Utah, mining area. Economic Geology, 78, 675-687.
Qiu, F., Abdelsalam, M., Thakkar, P. (2006). Spectral analysis of ASTER data covering part of the Neoproterozoic Allaqi-Heiani suture, Southern Egypt. Journal of African Earth Sciences 44, 169–180.
Rahaman, M. A. (1976). Review of the basement complex of Nigeria in: Kogbe, C. A. (ed) Geology of Nigeria. *Elizabethan publishing Lagos, Nigeria, 514.*
Rahaman, M.A. (1988). Recent advances in the study of the basement complex of Nigeria. *In: Geological Survey of Nigeria (ed) Precambrian Geology of Nigeria, pages 11–43.*
Ramadan, T.M., Abdelsalam, M.G., and Stern, R.J. (2001). Mapping gold-bearing massive sulfide deposits in the neoproterozoic Allaqi Suture, Southeast Egypt with Landsat TM and SIR-C/X SAR images; *Photogrammetric Engineering and Remote Sensing* 67(4) 491–497.
Ramadan, T.M. and Kontny, A. (2004). Mineralogical and structural characterization of alteration zones detected by remote sensing at Shalatein District, SE Desert, Egypt; *Journal of African Earth Sci.* 40 89–99.
Rowan, L.C. and Bowers, T.L. (1995). Analysis of linear features mapped in Landsat Thematic Mapper and side-looking airborne radar images of the Reno, Nevada 1 ° by 2 ° quadrangle, Nevada-implications for mineral resource studies. Photogrammetric Engineering and Remote Sensing, Volume 61, 749-759.
Sabins, F.F., 1999. Remote sensing for mineral exploration. Ore Geology Reviews 14, 157–183.
Salem, S.A. (2007). Using Remote Sensing Techniques in Geology and gold mineralization at al Faw - Eqat area, South Eastern Desert, Egypt, Egyptian Journal of Remote Sensing and Space Scien, 10: 137-150
Talaat, M.R and Mohammed, F.A. (2010). Characterization of gold mineralization in Garin Hawal area, Kebbi State, NW Nigeria, using remote sensing. The Egyptian Journal of Remote Sensing and Space Science. Volume 13, Issue 2, Pages 153–163.
Turner, D.C. (1983). Upper Proterozoic schist belts in the Nigerian sector of the Pan-African Province of West Africa. *Precambrian Res 21:55–79.*
Weissbeod T., Karcz I., Abed A., (1988), Discussion on the supposed Precambrian palaeosuture along the Dead Sea Rift , journal of the Geological Society, volume 142, number 3, 527-531.
Yousif, M.S.M. and Shedid, G.A. (1999). Remote sensing signature of some selected basement rock units from the central eastern desert of Egypt.Egypt. Journal of Remote Sensing and space Sci, vol. 1, 132-141.
Zoheir, B. and Emam, A. (2012). Integrating geologic and satellite imagery data for highresolution mapping and gold exploration targets in the South Eastern Desert, Egypt. Journal of African Earth Sciences 66–67.